HHS Public Access

Author manuscript

Biochem Biophys Res Commun. Author manuscript; available in PMC 2018 August 26.

Published in final edited form as:

Biochem Biophys Res Commun. 2017 August 26; 490(3): 1074–1079. doi:10.1016/j.bbrc.2017.06.168.

Tyro3 Carboxyl Terminal Region Confers Stability and Contains the Autophosphorylation Sites

Hanshuang Shao[1], **Douglas Lauffenburger**[3], and **Alan Wells**[1,2]

[1]Department of Pathology, University of Pittsburgh, Pittsburgh, PA 15213

[2]Pittsburgh VA Health System, Pittsburgh, PA 15213

[3]Department of Biological Engineering, MIT, Cambridge, MA 02319

Abstract

Tyro3, a member of TAM receptor tyrosine kinase family has been suggested to be autophosphorylated upon activation. In the current study we mapped the autophosphorylation sites of murine Tyro3 to tyrosine 723 and 756, with K540 being required for its kinase activity. Knockdown of Axl significantly decreases the tyrosyl-phosphorylation of Tyro3 in fibroblasts NR6WT, suggesting an interaction among the TAM family members. Interestingly, the carboxyl terminal region of Tyro3 is required for its stability in cells with a minimal length of 1-778 amino acids which is not conserved in murine Axl, a member of TAM. These data suggest that the autophosphorylation sites of TAM RTK members are unique although they share high similarity in amino acids within their carboxyl kinase domain.

Keywords

Tyro3; autophosphorylation; stability

1. Introduction

Tyro3, Axl, and MerTK comprise a receptor tyrosine kinase family (TAM) which has been implicated in cell proliferation, survival, migration and tumor angiogenesis upon stimulation by extracellular phospholipid ligands such as GAS6 [1];[2];[3];[4];[5];[6]. Abnormal expression of Axl and MerTK has been widely reported in many cancer cells [7];[8];[9];[10];[11]. Compared to Axl and MerTK, Tyro3 is the least studied although recently accumulating evidence revealed that the expression of Tyro3 is elevated in several cancer cells such as ovarian cancer, hepatocellular carcinoma, colon cancer and melanoma [12];[13];[14];[15];[16]. For example, Lee reported that overexpression of Tyro3 leads to a resistance in ovarian cancer cells to chemotherapeutic drug taxol [12]. Thus Tyro3 is being

Corresponding Author: Alan Wells, University of Pittsburgh School of Medicine, 3550 Terrace Street, S713 Scaife Hall, Pittsburgh, PA 15261. Phone: 412-647-8409; Fax: 412-624-8946; wellsa@upmc.edu.

considered as a potential therapeutic target in patients with cancer. To this point, we have found that Tyro3 can promote invasiveness of melanoma cells {Shao, 2017, submitted}. How these kinases actuate signal transduction downstream from the membrane is still ill-defined.

The three TAM family members share three types of conserved domains including two extracellular fibronectin type III (FNIII), two immunoglobulin-like domains and a unique kinase domain. The TAM family contains a conserved sequence, KW (I/L)A(I/L)ES which does not exist within the kinase domain of other RTKs [17]. Ligand binding to RTK receptors induces receptor dimerization and subsequent trans-autophosphorylation of tyrosine residues within the intracellular domain of RTK receptors which results in an increase of catalytic efficiency so that other substrates can be phosphorylated and a recruitment of signaling molecules containing SH2, PTB, or other phosphotyrosine-binding domains to docking sites of tyrosine-phosphorylated RTKs and other proteins. Human MerTK autophosphorylates at Y749, Y753 and Y754 [18]. By analogy, the tyrosines at Y779, Y821 and Y866 have been proposed as potential autophosphorylation sites of human Axl although there were no clear evidence to support that these three tyrosine residues are indeed autophosphorylation sites [19]. The autophosphorylation sites of Tyro3 have been suggested to localize within its C-terminal region [20]. In the present study, we identified Y723 and Y756 as two novel autophosphorylation sites of murine Tyro3. Importantly, we also found that Tyro3 stability is conferred by the domain beyond the autophosphorylation sites, suggesting a mechanism by which tumor-associated signaling could be regulated.

2. Materials and Methods

2.1. Cell culture and reagents

Fibroblasts NR6WT were cultured in alpha-MEM media supplemented with 1x sodium pyruvate, 1x non-essential amino acids, 1x pen/strep antibiotics, 1x L-glutamine, and 7.5% fetal bovine serum. Melanoma cell line WM1158 was cultured in DMEM (1 gL^{-1} glucose): L15 3:1 medium supplemented with 10% fetal bovine serum and 1x pen/strip antibiotics. Transfection reagent xFect was purchased from Clonetech Life Technologies (Grand Island, NY). Monoclonal phospho-tyrosine antibody (p-Tyr-100) was purchased from Cell Signaling Technology (Beverly, MA). GFP-Trap A beads used for immunoprecipitation of GFP-tagged protein were purchased from ChromoTek GmbH Planegg-Martinsried, Germany). Polyclonal GFP was purchased from Santa Cruz (Dallas, TA). Monoclonal GAPDH antibody was purchased from Sigma Aldrich (St. Louis, MO). Accuprime DNA polymerase supermix was purchased from Invitrogen (Life Technologies, Grand Island, NY).

2.2. Total RNA isolation

Fibroblasts NR6WT transfected with WT or truncated Tyro3 were grown to about 90% confluency prior to transfecting with WT or truncated Tyro3-eGFP. After transfection for 24hr, total RNA was extracted using Trizol reagents (Life Technologies, Grand Island, NY) according to the manufacturer's manual. The RNA pellet was finally reconstituted in sterile Milli-Q water and the concentration of total RNA was determined using spectrometry.

2.3. Quantitative PCR analysis

Quantitative PCR was performed in 25 μl reaction volume containing following components: 50 ng total cDNA, forward and reverse primers (250 nM each), and 1x SYBR® Green PCR Master Mix (Applied Biosystems Inc., Carlsbad, CA). The PCR mixture was then pre-denatured at 95°C for 5 min followed by 35 cycles of 30 seconds at 95°C, 30 seconds at 60°C, and 1 min at 72°C using Stratagene Mx3000P qPCR machine. Quantitative PCR data for target genes were normalized to the expression levels of GAPDH.

2.4. Cloning and mutagenesis

cDNA was synthesized using SuperScript® III First-Strand Synthesis SuperMix (Life Technologies, Grand Island, NY) according to the manufacturer's manual. Murine full length cDNAs of Tyro3 and Axl were amplified using polymerase chain reaction (PCR) and then were cloned into the expression vector pEGFP-N1. Mutagenesis of Tyro3 and Axl was performed using a previously described method [21]. All clones and mutagenesis were confirmed by DNA sequencing analyses.

2.5. Transfection

Cells were plated in regular six-well tissue culture plate in complete growth medium at a density to achieve ~90% confluency next day. To form a DNA-polymer complex, 4μg of endotoxin-free plasmid was diluted into 100 μl xFect reaction buffer and vortexed rigorously for 5 seconds prior to adding 1.5 μl of xFect polymer. The mixture was immediately vortexed at highest speed for 10 seconds and incubated for 10 minutes at room temperature without disturbance. During incubation, the complete cell culture medium was replaced with warm quiescence medium (0.1% dialyzed FBS for fibroblasts NR6Wt and 2% for Wm1158). Finally, the DNA-polymer mixture was slowly dropped into cell culture medium while the plate was rocked back and forth. Cells were further incubated at 37°C in a humidified incubator with 5% CO_2 for at least 16 hours prior to further analyses.

2.6. Immunoprecipitation

Culture plates were rinsed with cold PBS without calcium and magnesium prior to adding RIPA buffer in the presence of 1x protease inhibitors cocktails set V (Billerica, MA). Then cell debris were removed by rubber policeman and the cell lysate was transferred to a microcentrifugation tube for further incubation on ice for 5 min prior to spinning down (top speed in a microcentrifuge) at 4°C for 30 min. After centrifugation, the supernatant was transferred to a new microcentrifugation tube and incubated with GFP-Trap A beads at 4°C for 16h. Agarose beads were then spun down and completely washed with RIPA buffer followed by eluating with 2x SDS protein sample buffer. The eluted supernatant was finally boiled for 3 min. The eluted proteins were subjected to electrophoresis and immunoblotting.

2.7. Immunoblotting

Cells were washed briefly with PBS in the absence of calcium and magnesium and lysed in RIPA buffer in the presence of 1x protease inhibitors cocktails set V. The lysate was further incubated on ice for 5 min prior to sonicating briefly. After centrifugation at 4°C for 30 min, the supernatant was collelcted. The concentration of total protein was determined using

Thermo Scientific™ Pierce™ BCA™ Protein Assay (Rockland, IL). Ten micrograms of total proteins was mixed with 6x SDS sample buffer in the presence of β-mercaptoethanol and then was boiled for 3 min prior to loading on SDS-polymerized gel. After electrophoresis, proteins were transferred to a polyvinylidene difluoride (PVDF) membrane and immunoblotted with appropriate primary antibodies according to standard immunoblotting protocols.

3. Results

3.1. Mapping of Tyro3 kinase domain

The autophosphorylation of TAM receptors has been previously reported [18];[19]. Braunger et al. revealed that replacement of lysine with an arginine in the ATP binding pocket of human Axl (K567 > R567) quenched its autophosphorylation in 293 cells [19]. By aligning the amino acids sequence of human Axl and murine Tyro3, we found that human Axl K567 maps to murine Tyro3 K540. However, previous reports have K536 being designated the ATP binding site of murine Tyro3 in Rat2 cells [22]. Therefore, we tested whether the designated K536 or the nearby mapped K540 is the key ATP binding site of murine Tyro3 in fibroblasts NR6WT, in which Axl is expressed at higher level but only a trace of Tyro3 (Figure 1A). We first created a Tyro3 mutant K536M. Interestingly, we found that K536M autophosphorylated at a similar level with WT Tyro3 suggesting that K536 is not the ATP binding site of murine Tyro3 in fibroblasts NR6WT (Figure 1B top panel lane 2 vs lane 1). To ensure this was not an artifact of the methionine being able to stabilize the ATP binding pocket, we created K536R as arginine also has been commonly used to replace K to quench the ATP binding. As shown in Figure 1B (top panel, lane 3), K536R also was autophosphorylated suggesting that K536 is not the ATP binding site of Tyro3 in NR6WT. Next, we generated K540R and K540M and found that neither mutant was autophosphorylated in NR6WT (Figure 1B top panel lane 4 and lane 5), suggesting that the K540 is the ATP binding site of murine Tyro3 in NR6WT.

The selection of ATP-binding site may be cell type specific. Thus, we detected the autophosphorylation of K540R and K540M in melanoma cell line WM1158. As shown in Figure 1C, there was no detectable autophosphorylation of K540R and K540M in WM1158. To further confirm the autophosphorylation of both K536M and K536R was not due to species of cell type, we expressed K536M and K536R in WM1158 and found that both K536M and K536R were autophosphorylated at a similar level with WT Tyro3 (Figure 1D top panel Lane 2 and 3 vs lane 1). These data suggested that K540 is the ATP docking site of murine Tyor3 and the ATP binding to K540 of murine Tyro3 is not cell type-dependent.

Notably, Tyro3 usually presents two bands based due to posttranslational modifications such as glycosylation, ubiquitination and phosphorylation [17]. Surprisingly, we found that abolishment of autophosphorylation resulted in accumulation of the larger band compared to WT, suggesting that K540R/M is easily modified and even more stable than WT (last two lanes in Figure 1B bottom panel and 1C middle panel).

3.2. Mapping autophosphorylation site of Tyro3

The exact autophosphorylation sites of murine Tyro3 remain unknown although the autophosphorylation sites of Tyro3 have been suggested to localize within its C-terminal region [20]. To map the autophosphorylation sites of murine Tyro3, we first truncated the sequence after tyrosines sequentially from its C-terminal tail. As shown in Figure 2A, truncated mutant 1-839 Tyro3 and 1-793 Tyro3 were autophosphorylated at a similar level as full length but the other more severely truncated mutants had no detectable autophosphorylation. Truncation to 755, leaving Tyro3 without potential autophosphorylation site Y756 failed to be autophosphorylation suggesting that the Y756 is the autophosphorylation site of murine Tyro3. To further confirm Y756 as an autophosphorylation site of Tyro3, we replaced Y756 with phenylalanine (F) in the full length construct. Surprisingly, Y756F was still autophosphorylated to a similar extent as WT Tyro3 suggesting that Y756 is either not the autophosphorylation site or that there is another site besides Y756. Indeed, after creating a series of Tyro3 double phenylalanines (Y756F plus additional F substitutions) we finally found that Y756/723F was no longer autophosphorylated (Figure 2B). These data suggest that the Y723 and Y756 are the autophosphorylation sites of murine Tyro3. Based on previous studies and our current finding, the autophosphorylation sites of Tyro3, Axl and MerTk are unique although the amino acids in kinase domain of TAM are highly conserved suggesting that each TAM member might be specifically activated depending on different environmental stimuli and thus plays a district role.

Brown et al. [22] revealed that Axl closely interacts with Tyro3 in Rat2 cells in which Tyro3 is overexpressed. As Axl is highly expressed in the NR6WT fibroblasts (Figure 1A), we determined if reducing Axl by siRNA (Figure 2C) affects the phosphorylation of overexpressed Tyro3 in NR6WT. As shown in Figure 2D (lane 3 vs lane 1), downregulation of Axl expression diminishes the phosphorylation of exogenous Tyro3 suggesting Axl is involved in Tyro3 phosphorylation. To further confirm if the kinase activity of TAM family kinases is required for its autophosphorylation, we treated Tyro3 overexpressed NR6WT cells with R428, a selective TAM inhibitor. As expected, R428 significantly abolished the phosphorylation of Tyro3 in both control and Axl siRNA transfected NR6WT cells (Figure 2D lane 2 vs lane 4). Furthermore, the autophosphorylation of TAM, at least for Tyro3 is required for its role in phosphorylating other proteins such as alpha-actinin-4, a member of actin filaments cross-linking protein (Figure 2E).

3.3. The carboxyl tail of Tyro3 is required for its stability

During the identification of autophosphorylation sites of murine Tyro3, we observed that the protein level of 1-722 Tyro3 is dramatically decreased compared to full length and 1-793 Tyro3 suggesting that the carboxyl tail of Tyro3 might be required for maintaining the stability of Tyro3 (data not shown). To confirm this, we constructed a series of carboxyl truncated Tyro3 mutants and examined their stability in fibroblasts NR6WT. As shown in Figure 3A, the protein level appeared to vary with the extent of truncation of the carboxyl tail. This might occur at the protein or transcription level. Quantitative RT PCR analysis found no significant difference in mRNA among full length, or the extensively truncated 1-793 and 1-755 variants (Figure 3B). To probe protein degradation, we treated cells

transfected with full length, 1-793 and 1-755 with different concentrations of lactacystin, a proteasome inhibitor, for 18h prior to protein analysis by immunoblotting. As shown in Figure 3C, lactacystin significantly stabilized 1-755. These results suggest that the carboxyl tail is required for maintaining the stability of Tyro3.

To determine the minimal length which is required for maintaining the stability of Tyro3 we further constructed 1-780, 1-770 and 1-760 and found that 1-780 was expressed at similar level as full length and 1-793, but the expression levels of 1-770 and 1-760 significantly declined suggesting the minimal length was between 770–780 (Figure 3D). To finely map the exact length, we truncated Tyro3 starting from 1-784 one by one amino acid until 1-772. As shown in Figure 3E, 1-779 and longer mutants all expressed similar level as full length but the protein levels of 1-778 and all shorter mutants were degraded. Murine Tyro3 and Axl present very high identity in amino acids within their kinase domains. Therefore, we next determined whether the carboxyl tail of Axl is also required for its stability in NR6WT. As shown in Figure 3F, truncated mutants were expressed at a similar level with full length of Axl suggesting that the role of the carboxyl tail of Tyro3 in maintaining the stability of intact protein is not conserved among TAM receptors. Taken together, these results suggested that Tyro3 required 1-779 amino acids in length to maintain its stability.

4. Discussion

Herein, we mapped the phosphorylation functional sites of the receptor protein tyrosine kinase Tyro3. We found that the ATP acceptor is the second one in the nucleoside binding pocket, and that autophosphorylation occurs on two tyrosines in the unique carboxyl terminal region after the kinase domain, at Y723 and Y756. It should be noted that we did not demonstrate intra-molecular autophosphorylation per se, but rather tyrosyl-phosphorylation that occurs upon forced overexpression. That this was dependent on the Tyro3 kinase activity was demonstrated by elimination upon replacement of the acceptor lysine at position K540 with either arginine or methionine, and the inhibition by the TAM-selective inhibitor R428 [23]. It has been suggested that Tyro3 can be cross-phosphorylated by the related family member Axl, which is also expressed at high levels in NR6WT (Figure 1A). Indeed, our data revealed that siRNA downregulation of Axl significantly reduced phosphorylation of Tyro3. These data suggest that TAM family kinases coordinate for activation.

Interestingly, we find that simply over-expressing Tyro3 leads to tyrosyl-phosphorylation. Typically, activation of RTKs occurs by binding of ligand to their extracellular domains [24]. The vitamin K-dependent protein Gas6 was suggested to bind to Axl and Tyro3 with roughly equal affinity [25] although it was first identified as a ligand for Axl [26];[17]. Therefore, we attempted to determine if Gas6 treatment enhances the phosphorylation of overexpressed Tyro3 in NR6WT but failed (data not shown). The reasons are probably due to: a) phosphorylation of Tyro3 by Gas6 needs the involvement of additional cofactor that does not exist in NR6WT cells; b) in some cases, ligand-independent receptor activation can occur [17]; c) autophosphorylation of Tyro3 triggered by its intracellular kinase activity is constitutive even though when cells are starved with quiescence medium (only containing 0.1% dialyzed fetal bovine serum) for 24h. To exclude the probability of inactivity of Gas6

used in our experiments, we performed a traditional scratch assay and found that Gas6 significantly enhanced cell migration of NR6WT (data not shown).

The autophosphorylation sites all occur close after the kinase domain. This leaves open the question of other functional domains in the ~130 amino acids that follow this distal tyrosine. While there may be sites for cross-phosphorylation by other kinases, such EGFR {Shao et al, 2017 submitted}, or docking/protein interaction sites, we found that immediately distal to the tyrosine kinases is a stability domain. Removal of the next 40 amino acids destabilizes the protein, so that it is degraded by proteasomes. This would suggest an irreversible means for attenuating this potentially oncogenic signaling. If the autophosphorylation opens Tyro3 to protein interactions to enable signaling, it also would expose potential protease sites that would then direct the active Tyro3 towards proteosomal removal. As the activity of intracellular signaling proteases such as members of the calpain [21];[27] and caspase [28]; [29] families are localized within the cell, this could enable the activity of Tyro3 to be restricted to discrete subcellular areas. This suggests a mechanism by which blebbing can be controlled during amoeboid motility.

Supplementary Material

Refer to Web version on PubMed Central for supplementary material.

Acknowledgments

This work was supported, in whole or in part, by grants from the National Institutes of Health (NIGMS). The Pittsburgh VA provided in kind support.

References

1. Allen MP, Zeng C, Schneider K, Xiong X, Meintzer MK, Bellosta P, Basilico C, Varnum B, Heidenreich KA, Wierman ME. Growth arrest-specific gene 6 (Gas6)/adhesion related kinase (Ark) signaling promotes gonadotropin-releasing hormone neuronal survival via extracellular signal-regulated kinase (ERK) and Akt. Mol Endocrinol. 1999; 13:191–201. [PubMed: 9973250]
2. Allen MP, Linseman DA, Udo H, Xu M, Schaack JB, Varnum B, Kandel ER, Heidenreich KA, Wierman ME. Novel mechanism for gonadotropin-releasing hormone neuronal migration involving Gas6/Ark signaling to p38 mitogen-activated protein kinase. Mol Cell Biol. 2002; 22:599–613. [PubMed: 11756555]
3. Funakoshi H, Yonemasu T, Nakano T, Matumoto K, Nakamura T. Identification of Gas6, a putative ligand for Sky and Axl receptor tyrosine kinases, as a novel neurotrophic factor for hippocampal neurons. J Neurosci Res. 2002; 68:150–160. [PubMed: 11948660]
4. Fridell YW, Villa J Jr, Attar EC, Liu ET. GAS6 induces Axl-mediated chemotaxis of vascular smooth muscle cells. J Biol Chem. 1998; 273:7123–7126. [PubMed: 9507025]
5. Lee HJ, Jeng YM, Chen YL, Chung L, Yuan RH. Gas6/Axl pathway promotes tumor invasion through the transcriptional activation of Slug in hepatocellular carcinoma. Carcinogenesis. 2014; 35:769–775. [PubMed: 24233839]
6. Shiozawa Y, Pedersen EA, Patel LR, Ziegler AM, Havens AM, Jung Y, Wang J, Zalucha S, Loberg RD, Pienta KJ, Taichman RS. GAS6/AXL axis regulates prostate cancer invasion, proliferation, and survival in the bone marrow niche. Neoplasia. 2010; 12:116–127. [PubMed: 20126470]
7. Meyer AS, Miller MA, Gertler FB, Lauffenburger DA. The receptor AXL diversifies EGFR signaling and limits the response to EGFR-targeted inhibitors in triple-negative breast cancer cells. Sci Signal. 2013; 6:ra66. [PubMed: 23921085]

8. Scaltriti M, Elkabets M, Baselga J. Molecular Pathways: AXL, a Membrane Receptor Mediator of Resistance to Therapy. Clin Cancer Res. 2016; 22:1313–1317. [PubMed: 26763248]
9. Zhou L, Liu XD, Sun M, Zhang X, German P, Bai S, Ding Z, Tannir N, Wood CG, Matin SF, Karam JA, Tamboli P, Sircar K, Rao P, Rankin EB, Laird DA, Hoang AG, Walker CL, Giaccia AJ, Jonasch E. Targeting MET and AXL overcomes resistance to sunitinib therapy in renal cell carcinoma. Oncogene. 2016; 35:2687–2697. [PubMed: 26364599]
10. Brand TM, Iida M, Stein AP, Corrigan KL, Braverman CM, Luthar N, Toulany M, Gill PS, Salgia R, Kimple RJ, Wheeler DL. AXL mediates resistance to cetuximab therapy. Cancer Res. 2014; 74:5152–5164. [PubMed: 25136066]
11. Yumoto K, Eber MR, Wang J, Cackowski FC, Decker AM, Lee E, Nobre AR, Aguirre-Ghiso JA, Jung Y, Taichman RS. Axl is required for TGF-beta2-induced dormancy of prostate cancer cells in the bone marrow. Sci Rep. 2016; 6:36520. [PubMed: 27819283]
12. Lee C. Overexpression of Tyro3 receptor tyrosine kinase leads to the acquisition of taxol resistance in ovarian cancer cells. Mol Med Rep. 2015; 12:1485–1492. [PubMed: 25815442]
13. Duan Y, Wong W, Chua SC, Wee HL, Lim SG, Chua BT, Ho HK. Overexpression of Tyro3 and its implications on hepatocellular carcinoma progression. Int J Oncol. 2016; 48:358–366. [PubMed: 26573872]
14. Chien CW, Hou PC, Wu HC, Chang YL, Lin SC, Lin SC, Lin BW, Lee JC, Chang YJ, Sun HS, Tsai SJ. Targeting TYRO3 inhibits epithelial-mesenchymal transition and increases drug sensitivity in colon cancer. Oncogene. 2016; 35:5872–5881. [PubMed: 27132510]
15. Zhu S, Wurdak H, Wang Y, Galkin A, Tao H, Li J, Lyssiotis CA, Yan F, Tu BP, Miraglia L, Walker J, Sun F, Orth A, Schultz PG, Wu X. A genomic screen identifies TYRO3 as a MITF regulator in melanoma. Proc Natl Acad Sci U S A. 2009; 106:17025–17030. [PubMed: 19805117]
16. Demarest SJ, Gardner J, Vendel MC, Ailor E, Szak S, Huang F, Doern A, Tan X, Yang W, Grueneberg DA, Richards EJ, Endege WO, Harlow E, Koopman LA. Evaluation of Tyro3 expression, Gas6-mediated Akt phosphorylation, and the impact of anti-Tyro3 antibodies in melanoma cell lines. Biochemistry. 2013; 52:3102–3118. [PubMed: 23570341]
17. Linger RM, Keating AK, Earp HS, Graham DK. TAM receptor tyrosine kinases: biologic functions, signaling, and potential therapeutic targeting in human cancer. Adv Cancer Res. 2008; 100:35–83. [PubMed: 18620092]
18. Ling L, Templeton D, Kung HJ. Identification of the major autophosphorylation sites of Nyk/Mer, an NCAM-related receptor tyrosine kinase. J Biol Chem. 1996; 271:18355–18362. [PubMed: 8702477]
19. Braunger J, Schleithoff L, Schulz AS, Kessler H, Lammers R, Ullrich A, Bartram CR, Janssen JW. Intracellular signaling of the Ufo/Axl receptor tyrosine kinase is mediated mainly by a multi-substrate docking-site. Oncogene. 1997; 14:2619–2631. [PubMed: 9178760]
20. Graham DK, DeRyckere D, Davies KD, Earp HS. The TAM family: phosphatidylserine sensing receptor tyrosine kinases gone awry in cancer. Nat Rev Cancer. 2014; 14:769–785. [PubMed: 25568918]
21. Leloup L, Shao H, Bae YH, Deasy B, Stolz D, Roy P, Wells A. m-Calpain activation is regulated by its membrane localization and by its binding to phosphatidylinositol 4,5-bisphosphate. J Biol Chem. 2010; 285:33549–33566. [PubMed: 20729206]
22. Brown JE, Krodel M, Pazos M, Lai C, Prieto AL. Cross-phosphorylation, signaling and proliferative functions of the Tyro3 and Axl receptors in Rat2 cells. PLoS One. 2012; 7:e36800. [PubMed: 22606290]
23. Kimani SG, Kumar S, Bansal N, Singh K, Kholodovych V, Comollo T, Peng Y, Kotenko SV, Sarafianos SG, Bertino JR, Welsh WJ, Birge RB. Small molecule inhibitors block Gas6-inducible TAM activation and tumorigenicity. Sci Rep. 2017; 7:43908. [PubMed: 28272423]
24. Schlessinger J. Cell signaling by receptor tyrosine kinases. Cell. 2000; 103:211–225. [PubMed: 11057895]
25. Fisher PW, Brigham-Burke M, Wu SJ, Luo J, Carton J, Staquet K, Gao W, Jackson S, Bethea D, Chen C, Hu B, Giles-Komar J, Yang J. A novel site contributing to growth-arrest-specific gene 6 binding to its receptors as revealed by a human monoclonal antibody. Biochem J. 2005; 387:727–735. [PubMed: 15579134]

26. Stitt TN, Conn G, Gore M, Lai C, Bruno J, Radziejewski C, Mattsson K, Fisher J, Gies DR, Jones PF, et al. The anticoagulation factor protein S and its relative, Gas6, are ligands for the Tyro 3/Axl family of receptor tyrosine kinases. Cell. 1995; 80:661–670. [PubMed: 7867073]

27. Shao H, Chou J, Baty CJ, Burke NA, Watkins SC, Stolz DB, Wells A. Spatial localization of m-calpain to the plasma membrane by phosphoinositide biphosphate binding during epidermal growth factor receptor-mediated activation. Mol Cell Biol. 2006; 26:5481–5496. [PubMed: 16809781]

28. Adrain C, Creagh EM, Cullen SP, Martin SJ. Caspase-dependent inactivation of proteasome function during programmed cell death in Drosophila and man. J Biol Chem. 2004; 279:36923–36930. [PubMed: 15210720]

29. Andersson M, Sjostrand J, Petersen A, Honarvar AK, Karlsson JO. Caspase and proteasome activity during staurosporin-induced apoptosis in lens epithelial cells. Invest Ophthalmol Vis Sci. 2000; 41:2623–2632. [PubMed: 10937575]

Highlights

- Tyro3 carboxy terminus contains two autophosphorylation sites
- Long, unique carboxy terminus provides for Tyro3 protein stability

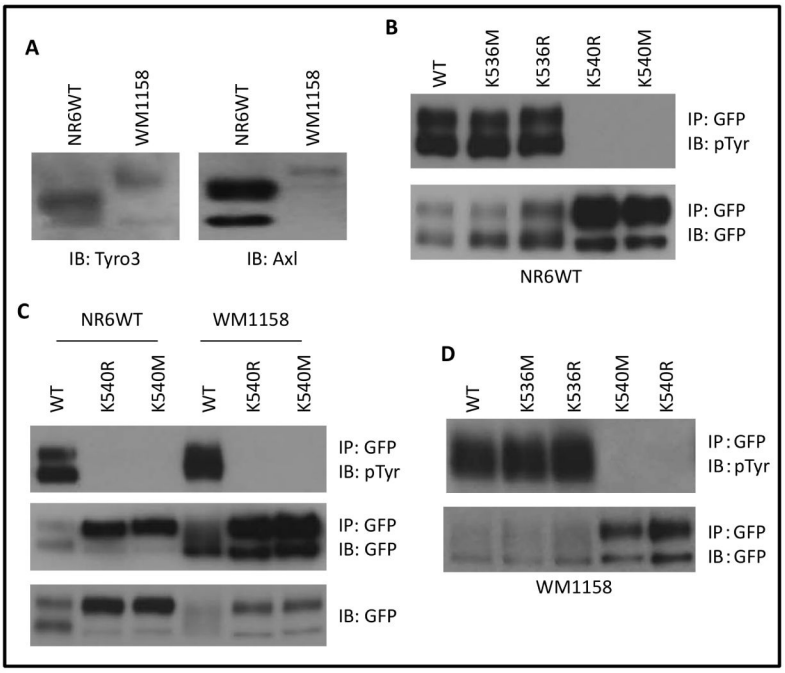

Fig. 1. K540 is required for autophosphorylation of Tyro3

(A) Immunoblotting of endogenous Tyro3 and Axl in fibroblasts NR6WT and melanoma WM1158 cells. (B) Immunoblotting of immunoprecipitated GFP-tagged proteins from fibroblasts NR6WT, with the indicated antibodies. (C) Immunoblotting of immunoprecipitated GFP-tagged proteins and total cell lysate of NR6WT and melanoma WM1158 cells transiently cotransfected with the indicated plasmids using the indicated antibodies. (D) Immunoblotting of immunoprecipitated GFP-tagged proteins from melanoma cells WM1158 with the indicated antibodies. Shown are representative images of three independent experiments.

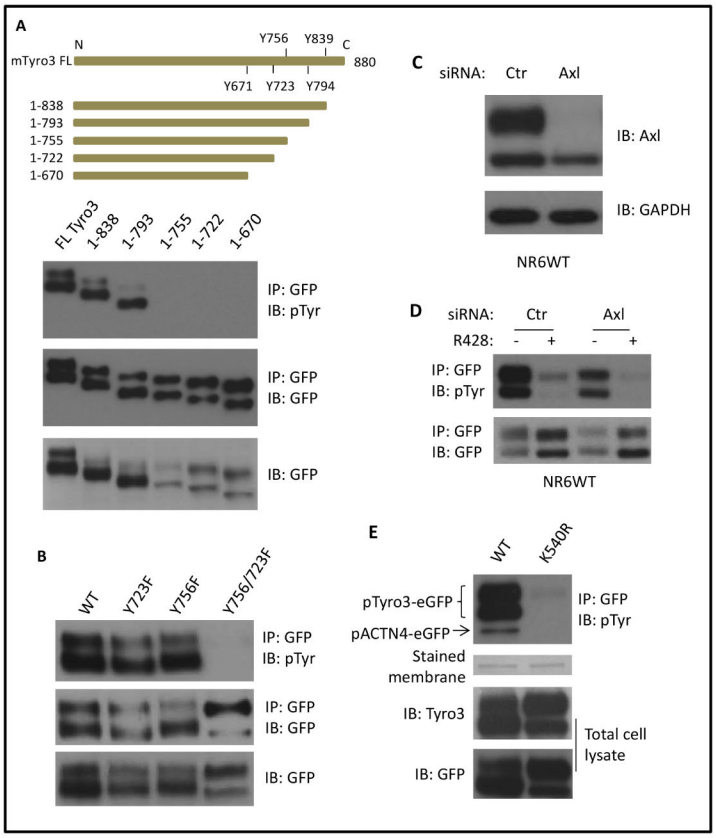

Fig. 2. Autophosphorylation of Tyro3 occurs at tyrosine 756 and 723

(A) Schematic of truncated Tyro3 and immunoblotting of immunoprecipitated and total cellular GFP-tagged truncated Tyro3 mutants using the indicated antibodies. **(B)** Immunoblotting of immunoprecipitated GFP-tagged proteins and total cell lysate of NR6WT cells transiently cotransfected with the indicated plasmids. **(C)** Immunoblotting of endogenous Axl of fibroblasts NR6WT transfected by murine Axl siRNA for 48h. (D) Immunoblotting of immunoprecipitated exogenous WT Tyro3-eGFP from fibroblasts NR6WT transfected with Axl siRNA for 24h followed by further transfection of WT Tyro3 plasmid. (E) Immunoblotting of immunoprecipitated GFP-tagged ACTN4 and total cellular GFP-tagged Tyro3. Stained membrane stands for PVDF membrane that was stained for protein. Shown are representative images of three independent experiments.

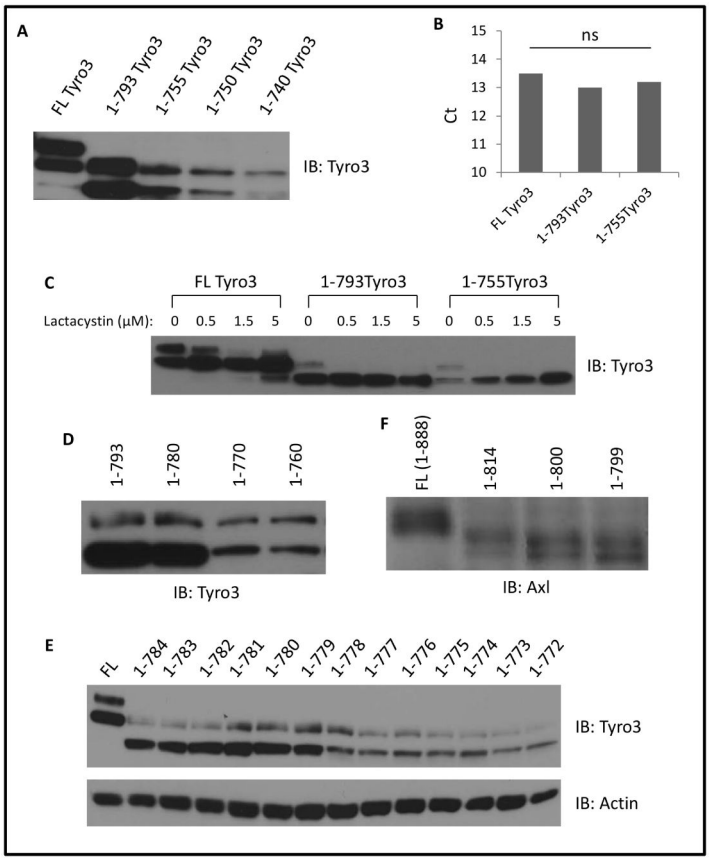

Fig. 3. Carboxyl terminal region of Tyro3 maintains its stability in fibroblasts NR6WT

(A) Tyro3 immunoblotting of total cell lysate of NR6WT fibroblasts transiently expressing the indicated Tyro3 truncated mutants. **(B)** Quantitative PCR analysis of truncated Tyro3 mutants in NR6WT fibroblasts. Data are mean ± SD of three independent experiments. Statistical analysis was performed using Student's t-test. ns: no statistical difference. **(C)** Tyro3 immunoblotting of total cell lysate of NR6WT fibroblasts transiently expressing Tyro3 truncated mutants and treated with the indicated concentration of lactacystin. **(D)** Tyro3 immunoblotting of the indicated truncated mutants. **(E)** Immunoblotting of total cell lysate of NR6WT fibroblasts expressing full length or truncated Tyro3. (F) Immunoblotting of total cell lysate of NR6WT fibroblasts expressing full length or truncated murine Axl. Shown are representative images of three independent experiments.